Draft version of March 5, 2003

HAMILTONIAN PARTICLE-MESH METHOD FOR TWO-LAYER SHALLOW-WATER EQUATIONS SUBJECT TO THE RIGID-LID APPROXIMATION

COLIN COTTER*, JASON FRANK†, AND SEBASTIAN REICH‡

Abstract. We develop a particle-mesh method for two-layer shallow-water equations subject to the rigid-lid approximation. The method is based on the recently proposed Hamiltonian particle-mesh (HPM) method and the interpretation of the rigid-lid approximation as a set of holonomic constraints. The suggested spatial discretization leads to a constrained Hamiltonian system of ODEs which is integrated in time using a variant of the symplectic SHAKE/RATTLE algorithm. It is demonstrated that the elimination of external gravity waves by the rigid-lid approximation can be achieved in a computationally stable and efficient way.

1. Introduction. Theorists frequently regard the ocean as a two-layer fluid with the interface between layers corresponding to the main thermocline. This idealization is perhaps most appropriate in the northwestern subtropical North Atlantic. Consider, then, a rotating fluid composed of two immiscible layers with different constant densities $\rho_1 < \rho_2$ over a flat bottom topography at $z = 0$. See Fig. 1.1 and the excellent exposition by SALMON [19]. Under the assumption that $\rho_1 \approx \rho_2$, the associated two-layer shallow-water equations are

$$\frac{D}{Dt_i}\mathbf{u}_i + f\mathbf{u}_i^\perp = \begin{cases} -g\nabla_{\mathbf{x}}(h_1+h_2), & i=1, \\ -g\nabla_{\mathbf{x}}(h_1+h_2) - g'\nabla_{\mathbf{x}}h_2, & i=2, \end{cases} \tag{1.1}$$

where $\mathbf{u}_i \equiv (u_i, v_i)^T$ is the horizontal velocity in the ith layer, $f > 0$ is the *Coriolis parameter*, $\mathbf{u}_i^\perp \equiv (-v_i, u_i)^T$,

$$\frac{D}{Dt_i} \equiv \frac{\partial}{\partial t} + \mathbf{u}_i \cdot \nabla_{\mathbf{x}}, \qquad \text{and} \qquad g' \equiv \frac{\rho_2 - \rho_1}{\rho_2} g$$

is the *reduced gravity*.[1] By assumption $g' \ll g$. Each layer-depth h_i satisfies the continuity equation

$$\frac{\partial h_i}{\partial t} + \nabla_{\mathbf{x}} \cdot (h_i \mathbf{u}_i) = 0. \tag{1.2}$$

It is also reasonable to assume that the combined flow in both layers is incompressible which leads to the *rigid-lid* constraint

$$h \equiv h_1 + h_2 = H = const. \tag{1.3}$$

and equation (1.1) is replaced by

$$\frac{D}{Dt_i}\mathbf{u}_i + f\mathbf{u}_i^\perp = \begin{cases} -\nabla_{\mathbf{x}}p, & i=1, \\ -\nabla_{\mathbf{x}}p - g'\nabla_{\mathbf{x}}h_2, & i=2, \end{cases} \tag{1.4}$$

where p is the pressure field enforcing the rigid-lid constraint (1.3) which, after differentiation in time, is equivalent to

$$\nabla_{\mathbf{x}} \cdot (h_1\mathbf{u}_1) + \nabla_{\mathbf{x}} \cdot (h_2\mathbf{u}_2) = 0.$$

*Department of Mathematics, Imperial College London, 180 Queen's Gate, London SW7 2AZ, United Kingdom, (e-mail: colin.cotter@imperial.ac.uk)

†CWI, P.O. Box 94079, 1090 GB Amsterdam, The Netherlands (e-mail: jason@cwi.nl)

‡ Department of Mathematics, Imperial College London, 180 Queen's Gate, London SW7 2AZ, United Kingdom (e-mail: s.reich@imperial.ac.uk)

[1] Eq. (1.1) is a slight variation of the formulation given by SALMON in [19] on page 85. While eq. (1.1) leads to a Hamiltonian formulation, no obvious Hamiltonian interpretation of the eq. (12.3) in [19] could be found. However, both formulations are identical under the rigid-lid approximation.

We also make the simplifying assumption that both layers have a (non-dimensionalized) *mean layer-depth* of $H_i = 1$, *i.e.* $H = H_1 + H_2 = 2$, and replace reduced gravity g' by an appropriate constant c_0.

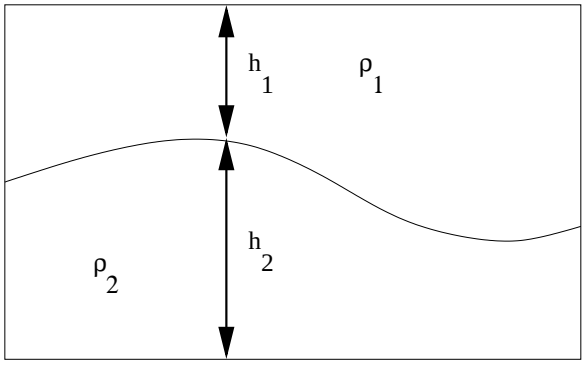

FIG. 1.1. *Two layer shallow-water model with rigid-lid.*

In a Lagrangian description of the model, we introduce a continuum of fluid particles $\mathbf{X}_i(\mathbf{a}_i, t) \equiv (X_i(\mathbf{a}_i, t), Y_i(\mathbf{a}_i, t))^T$ in each layer $i = 1, 2$, which are *labelled/marked* by their initial positions $\mathbf{a}_i = \mathbf{X}_i(\mathbf{a}_i, 0)$. Hence the independent variables are time t and labels $\mathbf{a}_i$. The material time derivative D/Dt becomes a partial derivative which, with a slight abuse of notation, we denote by d/dt.

Let $h_i^o(\mathbf{a}_i)$ denote the initial layer-depth at $t = 0$. Then the layer-depth is given at any time t by

$$h_i(\mathbf{x}, t) = \int h_i^o(\mathbf{a})\, \delta(\mathbf{x} - \mathbf{X}_i(\mathbf{a}_i, t))\, d^2\mathbf{a}_i, \qquad i = 1, 2, \tag{1.5}$$

where δ denotes the Dirac delta function. This formula and

$$\frac{d}{dt}\mathbf{X}_i = \mathbf{u}_i$$

replace the continuity equation (1.2) in a Lagrangian description of fluid dynamics. Hence we finally obtain the constrained infinite-dimensional Newtonian equations of motion

$$\begin{aligned}
\frac{d}{dt}\mathbf{u}_i &= -f\mathbf{u}_i^{\perp} - \begin{cases} \nabla_{\mathbf{X}_1} p, & i = 1, \\ \nabla_{\mathbf{X}_2} p + c_0 \nabla_{\mathbf{X}_2} h_2, & i = 2, \end{cases} \\
\frac{d}{dt}\mathbf{X}_i &= \mathbf{u}_i, \\
0 &= h_1(\mathbf{X}_1, t) + h_2(\mathbf{X}_2, t) - H.
\end{aligned}$$

In the following section we describe a spatial discretization for this model.

2. The Hamiltonian Particle-Mesh (HPM) Method with Rigid-Lid Constraint. To simplify the discussion we assume a double periodic domain $\mathbf{x} \in \mathcal{R} \equiv [-\pi, +\pi)^2$ and introduce a regular grid $\mathbf{x}^{pq}$ on $\mathcal{R}$ with equal grid spacing Δx in the x and y-direction. Let $\psi^{pq}(\mathbf{x})$ denote the tensor product cubic B-spline centered at $\mathbf{x}^{pq} \equiv (x^{pq}, y^{pq})^T$, *i.e.*

$$\psi^{pq}(\mathbf{x}) \equiv \psi_{\text{cs}}\left(\frac{x^{pq} - x}{\Delta x}\right) \cdot \psi_{\text{cs}}\left(\frac{y^{pq} - y}{\Delta x}\right),$$

where $\psi_{\rm cs}(r)$ is the cubic spline

$$\psi_{\rm cs}(r) \equiv \begin{cases} \frac{2}{3} - |r|^2 + \frac{1}{2}|r|^3, & |r| \le 1, \\ \frac{1}{6}(2-|r|)^3, & 1 < |r| \le 2, \\ 0, & |r| > 2 \end{cases}$$

These basis functions form a *partition of unity, i.e.*

$$\sum_{p,q} \psi^{pq}(\mathbf{x}) = 1.$$

Furthermore, we also have

$$\sum_{p,q} \nabla_{\mathbf{x}} \psi^{pq}(\mathbf{x}) = 0,$$

which is a desirable property when computing gradients. In each layer $i = 1, 2$, we introduce N discrete particles $\mathbf{X}_i^k$, $k = 1, \ldots, N$, with masses m_i^k such that[2]

$$h_i^o(\mathbf{x}^{pq}) \approx \sum_{k=1}^{N} m_i^k \, \psi^{pq}(\mathbf{X}_i^k)$$

at time $t = 0$. More specifically, we approximate the layer-depth h_2 on the grid by

$$h_2^{pq} \equiv \sum_{k=1}^{N} m_2^k \, \psi^{pq}(\mathbf{X}_2^k)$$

and the total layer-depth by

$$h^{pq}(\mathbf{X}) \equiv \sum_{k=1}^{N} \left(m_1^k \, \psi^{pq}(\mathbf{X}_1^k) + m_2^k \psi^{pq}(\mathbf{X}_2^k) \right),$$

where, for later use, we introduced the notation $h^{pq}(\mathbf{X})$ to indicate that h^{pq} depends on all particle positions $\mathbf{X}_i^k$ collected in the vector $\mathbf{X}$.

So far we have essentially followed the standard methodology for deriving *particle-mesh* (PM) methods [10, 4]. The following steps are crucial to the *Hamiltonian particle-mesh* (HPM) method as introduced by FRANK, GOTTWALD & REICH [7] for geophysical fluid dynamics simulations. Even though the layer-depth in rotating fluids often stays relatively smooth, the numerical approximations h_1^{pq} and h^{pq} will develop some non-smoothness in strongly mixing flows due to the finite number of particles used to resolve the fluid motion and this tends to destabilize PM methods. We suggested in [7] to apply a (discretized) smoothing operator

$$S = (1 - \alpha^2 \nabla_{\mathbf{x}}^2)^{-2} \tag{2.1}$$

over the fixed Eulerian grid $\mathbf{x}^{pq}$ with a smoothing length $\alpha = 2\Delta x$. Let us denote the resulting smoothed approximation to h_2^{pq} by $\hat{h}_2^{pq}$. While this idea works very well for compressible flows it cannot be used to enforce the incompressibility condition (1.3). Instead the following strategy proved successful. We introduce a meta-grid with grid-spacing $\Delta\bar{x} \equiv 2\Delta x$ and grid points denoted by $\bar{\mathbf{x}}^{mn}$. Let $\phi^{mn}(\mathbf{x})$ denote the associated tensor product B-spline centered at $\bar{\mathbf{x}}^{mn} \equiv (\bar{x}^{mn}, \bar{y}^{mn})^T$, *i.e.*

$$\phi^{mn}(\mathbf{x}) \equiv \psi_{\rm cs}\left(\frac{\bar{x}^{mn} - x}{\Delta\bar{x}}\right) \cdot \psi_{\rm cs}\left(\frac{\bar{y}^{mn} - y}{\Delta\bar{x}}\right),$$

[2] If the particles $\mathbf{X}_i^k$ are initially placed on a regular grid with equal spacing Δa in the x and y-direction, then, following (1.5), one can use $m_i^k \equiv h_i^o(\mathbf{X}_i^k)\,(\Delta a/\Delta x)^2$.

Then an averaged (coarse-grained) total layer-depth is defined by

$$\bar{h}^{mn}(\mathbf{X}) \equiv \frac{1}{4}\sum_{pq} \phi^{mn}(\mathbf{x}^{pq})\, h^{pq}(\mathbf{X}).$$

The discrete pressure approximation $\bar{p}^{mn}$ is also defined over the coarse grid $\bar{\mathbf{x}}^{mn}$ and the resulting total force acting on particle $\mathbf{X}_i^k$ (excluding the Coriolis contribution) is given by

$$\mathbf{F}_i^k(\mathbf{X}, \bar{\mathbf{p}}) \equiv -\sum_{p,q} \nabla_{\mathbf{X}_i^k} \psi^{pq}(\mathbf{X}_i^k) \times \begin{cases} \left(\sum_{m,n} \phi^{mn}(\mathbf{x}^{pq})\, \bar{p}^{mn}\right) & i = 1, \\ \left(c_0 \hat{h}_2^{pq} + \sum_{m,n} \phi^{mn}(\mathbf{x}^{pq})\, \bar{p}^{mn}\right) & i = 2, \end{cases}$$

where $\bar{\mathbf{p}}$ denotes the vector of pressure variables $\bar{p}^{mn}$. Another important aspect of the HPM method is that the forces are derived from an exact gradient. This implies a number of very desirable conservation properties such as conservation of circulation, potential vorticity (PV), total mass, and energy [8, 5]. We note that energy conserving variants of PM methods have been considered, for example, by Lewis [14] and Langdon [12] in the context of plasma physics simulations.

The discrete set of constrained Newtonian equations of motion is now

$$\frac{d}{dt}\mathbf{u}_i^k = -f_i^k J \mathbf{u}_i^k + \mathbf{F}_i^k(\mathbf{X}, \bar{\mathbf{p}}), \qquad J \equiv \begin{bmatrix} 0 & 1 \\ -1 & 0 \end{bmatrix}, \tag{2.2}$$

$$\frac{d}{dt}\mathbf{X}_i^k = \mathbf{u}_i^k, \tag{2.3}$$

$$0 = \bar{h}^{mn}(\mathbf{X}) - H, \tag{2.4}$$

for $i = 1, 2$ and $k = 1, \ldots, N$. Here f_i^k denotes the value of the Coriolis parameter at particle location $\mathbf{X}_i^k$. In the following, let us first assume that the Coriolis parameter f is constant, *i.e.* $f = f_0$. Later we will consider the more general case of variable f. Then (2.2)-(2.4) gives rise to a constrained Hamiltonian system with the $\bar{p}^{mn}$'s acting as Lagrange multipliers to enforce the *holonomic constraints* (2.4). The Hamiltonian is

$$\mathcal{H}(\mathbf{X}, \mathbf{v}, \bar{\mathbf{p}}) \equiv \sum_{i=1}^{2}\sum_{k=1}^{N} \frac{1}{2m_i^k}\mathbf{v}_i^k \cdot \mathbf{v}_i^k + \frac{c_0}{2}\sum_{p,q} \hat{h}_2^{pq}(h_2^{pq} - H_2) + \sum_{m,n}(\bar{h}^{mn} - H)\bar{p}^{mn},$$

with conjugate momenta $\mathbf{v}_i^k \equiv m_i^k \mathbf{u}_i^k$. The equations (2.2)-(2.4) are equivalent to

$$\begin{aligned} \frac{d}{dt}\mathbf{v}_i^k &= f_0 J \nabla_{\mathbf{v}_i^k}\mathcal{H} - \nabla_{\mathbf{X}_i^k}\mathcal{H}, \\ \frac{d}{dt}\mathbf{X}_i^k &= \nabla_{\mathbf{v}_i^k}\mathcal{H}, \\ 0 &= \nabla_{\bar{p}^{mn}}\mathcal{H}, \end{aligned}$$

$i = 1, 2$, $k = 1, \ldots, N$. The *symplectic two-form* [2] is given by

$$\omega \equiv \sum_{i,k}\left[d\mathbf{X}_i^k \wedge d\mathbf{v}_i^k + \frac{f_0}{2} d\mathbf{X}_i^k \wedge J^{-1} d\mathbf{X}_i^k\right], \tag{2.5}$$

which is preserved along solutions.

To actually find the pressure in terms of the given particle locations and velocities, one has to solve a linear system of equations of type

$$A\bar{\mathbf{p}} = \mathbf{b} \tag{2.6}$$

with the entries $a^{mn}_{m'n'}$ of A defined by

$$a^{mn}_{m'n'} \equiv \sum_{k,i,p,q,p',q'} \frac{m^k_i}{V} \phi^{mn}(\mathbf{x}^{pq}) \left(\nabla \psi^{pq}(\mathbf{X}^k_i) \cdot \nabla \psi^{p'q'}(\mathbf{X}^k_i) \right) \phi^{m'n'}(\mathbf{x}^{p'q'})$$

This looks like a horrendous computational exercise but we found that the matrix is sparse and needs to be computed only once and can then be used in a quasi-Newton method throughout the simulation. See the following section for details.

3. Symplectic Time-Stepping Algorithm. Following JAY [11] and REICH [15], we develop a variant of the popular SHAKE/RATTLE algorithm [1, 18, 13] for Hamiltonian systems with holonomic constraints. In particular, the following two steps are performed during each time-step:
Step 1.

$$\mathbf{u}^k_i(t_{n+1/2}) = \mathbf{u}^k_i(t_n) + \frac{\Delta t}{2} \left\{ f_0 J \mathbf{u}^k_i(t_{n+1/2}) + \mathbf{F}^k_i(\mathbf{X}(t_n), \bar{\mathbf{p}}(t_{n+1/2})) \right\}, \tag{3.1}$$

$$\mathbf{X}^k_i(t_{n+1}) = \mathbf{X}^k_i(t_n) + \Delta t \mathbf{u}^k_i(t_{n+1/2}), \tag{3.2}$$

$$0 = \bar{h}^{pq}(\mathbf{X}(t_{n+1})) - H, \tag{3.3}$$

which requires the solution of a nonlinear system in the pressure variable $\bar{\mathbf{p}}(t_{n+1/2})$ to satisfy the holonomic constraint (3.3).
Step 2.

$$\mathbf{u}^k_i(t_{n+1}) = \mathbf{u}^k_i(t_{n+1/2}) + \frac{\Delta t}{2} \left\{ f_0 J \mathbf{u}^k_i(t_{n+1/2}) + \mathbf{F}^k_i(\mathbf{X}(t_{n+1}), \bar{\mathbf{p}}(t_{n+1/2})) \right\}. \tag{3.4}$$

The scheme can be rewritten in terms of the canonical momenta $\mathbf{v}^k_i(t_n)$ and the method conserves the symplectic structure (2.5) from time-step to time-step, *i.e.*, the method is *symplectic* [20]. Backward error analysis [3, 9, 16] implies excellent conservation of energy.

If the Coriolis parameter f is not constant, then $f^k_i \equiv f(\mathbf{X}^k_i(t_n))$ is used in (3.1) and $f^k_i \equiv f(\mathbf{X}^k_i(t_{n+1}))$ in (3.4) instead of f_0.

The nonlinear system of equations in the pressure variable $\bar{\mathbf{p}}(t_{n+1/2})$ can be solved by the following quasi-Newton method. Let us denote the iteration index by $l \geq 0$. Then given some approximation $\bar{\mathbf{p}}^{[l]}$, we can compute the associated approximation to the vector of particle positions $\mathbf{X}(t_{n+1})$ using (3.1)-(3.2) with $\bar{\mathbf{p}}(t_{n+1/2}) = \bar{\mathbf{p}}^{[l]}$. The next pressure approximation

$$\bar{\mathbf{p}}^{[l+1]} \equiv \bar{\mathbf{p}}^{[l]} + \frac{\Delta t^2}{2} \Delta \mathbf{p}^{[l]}$$

is then found by solving (2.6) with $\bar{\mathbf{p}} = \Delta \mathbf{p}^{[l]}$ and $\mathbf{b} = -(\bar{h}^{pq}(\mathbf{X}(t_{n+1})) - H)$. The iteration matrix A is only computed once at the beginning of the simulation.

4. Barotropic and Baroclinic Motion. Let us introduce the continuous Eulerian velocity approximation

$$\mathbf{u}_1(\mathbf{x}, t) \equiv \frac{\sum_{k=1}^N \mathbf{u}^k_1(t) \psi^{pq}(\mathbf{X}^k_1(t))}{\sum_{k=1}^N \psi^{pq}(\mathbf{X}^k_1(t))}$$

for the first layer and

$$\mathbf{u}_2(\mathbf{x}, t) \equiv \frac{\sum_{k=1}^N \mathbf{u}^k_2(t) \psi^{pq}(\mathbf{X}^k_2(t))}{\sum_{k=1}^N \psi^{pq}(\mathbf{X}^k_2(t))}$$

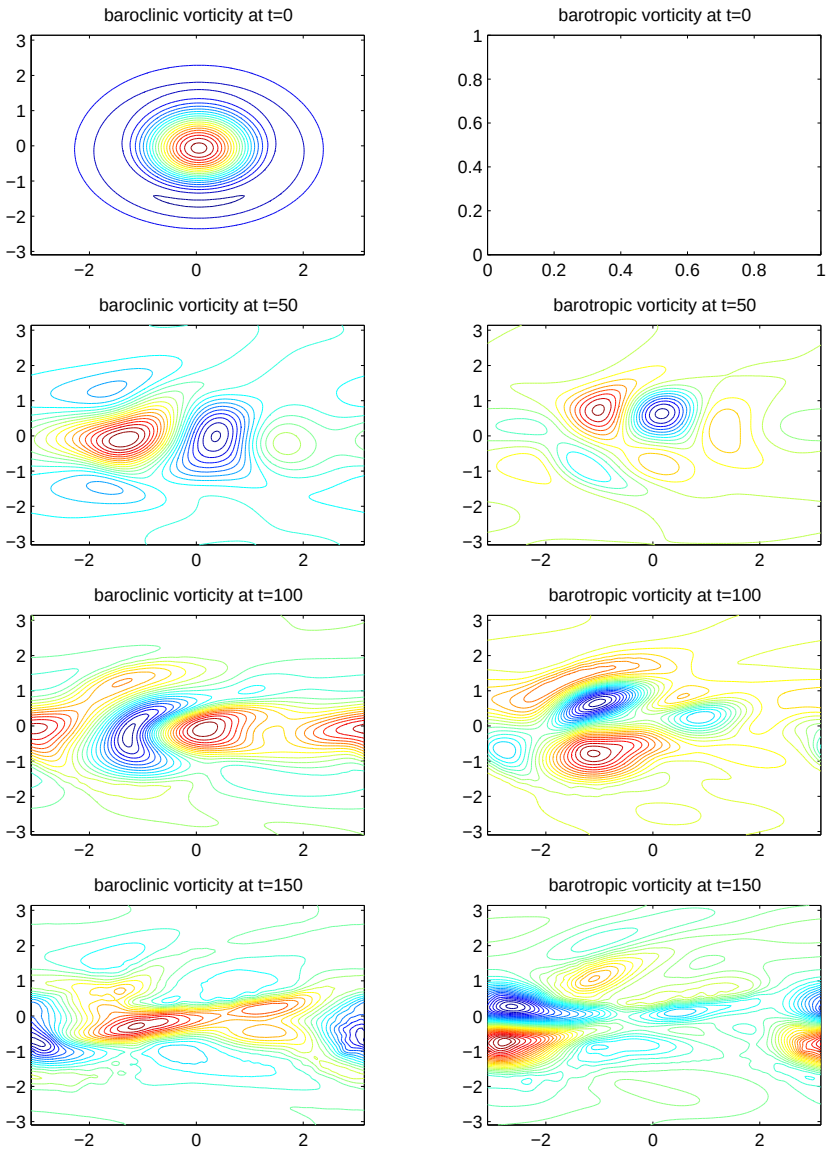

FIG. 3.1. *HPM simulation for shallow-water model with rigid-lid. Top to bottom: time evolution of vorticity; left: baroclinic vorticity; right: barotropic vorticity.*

for the second layer, respectively. Assuming again that $H_1 = H_2 = 1$, the *barotropic* velocity contribution to the flow is defined by

$$\mathbf{u}(\mathbf{x},t) \equiv \frac{1}{2}\left\{\mathbf{u}_1(\mathbf{x},t) + \mathbf{u}_2(\mathbf{x},t)\right\},$$

which represents synchronized motion in both layers, and the *baroclinic* mode by

$$\Delta\mathbf{u}(\mathbf{x},t) \equiv \frac{1}{2}\left\{\mathbf{u}_1(\mathbf{x},t) - \mathbf{u}_2(\mathbf{x},t)\right\},$$

which represents fluid motion pointing in opposite directions (the *thermal wind*).

If initially $\Delta\mathbf{u} = 0$ and $h_2 = H_2 = 1$, then the *available potential energy* (APE)

$$E_{\rm ap} \equiv \frac{c_0}{2} \sum_{p,q} \hat{h}_2^{pq} (h_2^{pq} - H_2)$$

is zero and the motion can be reduced to a purely barotropic single layer shallow-water model with a rigid-lid approximation (corresponding to an infinite Rossby deformation radius). On the contrary, $h_2 \neq H_2$ leads to baroclinic motion which is strongly dependent upon its length scale λ relative to the *internal Rossby deformation radius*

$$\lambda_{\rm int} \equiv \frac{\sqrt{c_0}}{f_0} \sqrt{\frac{H_1 H_2}{H_1 + H_2}} = \sqrt{\frac{c_0}{2 f_0^2}}.$$

For length-scales $\lambda \gg \lambda_{\rm int}$, most of the energy is stored in the layer-depth variation h_2 (*i.e.*, in the APE contribution to $\mathcal{H}$). This energy is eventually transformed into kinetic (barotropic) energy in a process called *baroclinic instability*. In this process the baroclinic modes are reduced to those of length-scale $\lambda \sim \lambda_{\rm int}$ unless external forcing leads to the activation of large scale variations in h_2 (such as tropical heating and polar cooling).

Another important concept is that of *geostrophic balance*. By this we mean that the velocities $\mathbf{u}_i$ in each layer stay close to their *geostrophic wind* approximations

$$\mathbf{u}_{{\rm gw},1} \equiv f_0^{-1} \nabla_{\mathbf{x}}^{\perp} p, \qquad \mathbf{u}_{{\rm gw},2} \equiv f_0^{-1} \nabla_{\mathbf{x}}^{\perp} (p + c_0 h_2)$$

if initialized appropriately. These two definitions imply in particular the balanced thermal wind relation

$$\Delta\mathbf{u}_{\rm thw} \equiv -\frac{c_0}{2 f_0} \nabla_{\mathbf{x}}^{\perp} h_2. \tag{4.1}$$

The associated *baroclinic stream function* $\tau \equiv -c_0/(2f_0) h_2$ represents the vertically averaged temperature anomaly of the fluid.

The *geostrophic approximation* is valid for small *Rossby number* flows, *i.e.*

$$Ro \equiv \frac{U}{\lambda f_0} \ll 1,$$

where U and λ are the typical velocity- and length-scales respectively, for the flow under consideration. For a precise scaling analysis see SALMON [19].

To be able to model *Rossby waves* within the framework of double periodic boundary conditions $\mathbf{x} = (x, y)^T \in \mathcal{R} \equiv [-\pi, +\pi)^2$, we defined a variable Coriolis parameter f by

$$f(y) \equiv f_0 + \beta \sin y.$$

Hence, near $y = 0$, we approximately reproduce a β-plane approximation $f \approx f_0 + \beta y$ and Rossby waves near $y = 0$ move westwards.

5. Numerical Experiments. We compute the solution starting from a purely baroclinic initial state defined by

$$\mathbf{u}_2 \equiv -\mathbf{u}_1 \equiv \frac{c_0}{2f} \nabla_{\mathbf{x}}^{\perp} (S h_2^o),$$

where $c_0 \equiv 1$, $f \equiv \sqrt{2}(1 + 0.2 \sin y)$,

$$h_2^o(\mathbf{x}) \equiv \frac{1}{1 + 0.08 \exp(-0.85 \|\mathbf{x}\|^2)} + \delta,$$

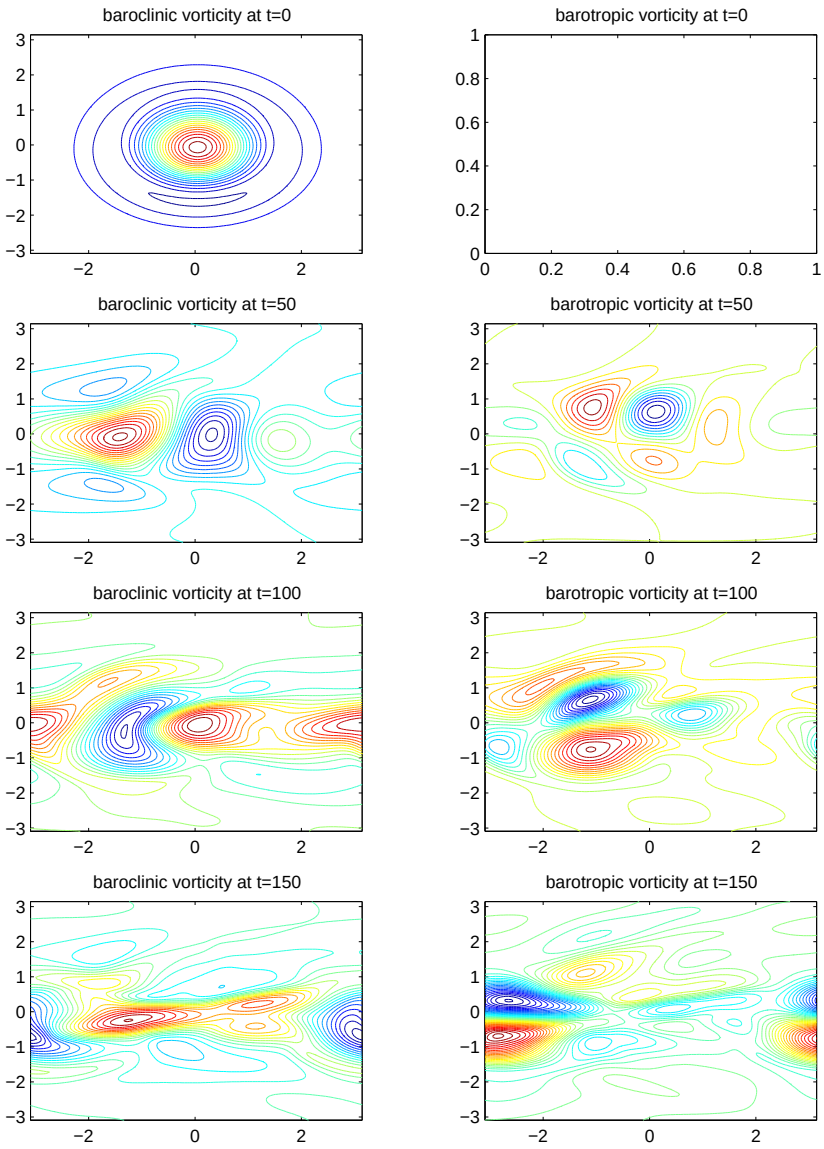

FIG. 4.1. *PS simulation for shallow-water model without rigid-lid. Top to bottom: time evolution of vorticity; left: baroclinic vorticity; right: barotropic vorticity.*

with the constant δ chosen such that h_2^{pq} has mean value equal to one. The initial state slowly moves westwards (along the negative x-axis) and breaks up into smaller (barotropic and baroclinic) vortices. The internal deformation radius is $\lambda_{\text{int}} = 0.5$.

The spatial grid resolution for the rigid-lid HPM method is $\Delta x = 2\pi/128 \approx 0.0491$ with $N = 147456$ particles per layer, i.e. $\Delta a = \Delta x/3$. The smoothing length in (2.1) is $\alpha = 2\Delta x \approx 0.0982$ and the operator S is implemented using FFT. We also implemented a pseudo-spectral (PS) method for the standard Eulerian formulation of the compressible two-layer shallow-water equations with $\Delta x = 2\pi/256 \approx 0.0245$ and a semi-implicit discretization in time (see [6]). The external deformation radius for the unconstrained shallow-water model is $\lambda_{\text{ext}} = 10$, *i.e.* $g' = g/400$.

Both methods were implemented using MATLAB, and *mex*-files were used for the particle-mesh computations within the HPM method. In terms of CPU time, one time-step with the constrained

HPM method takes about 5-10 times longer than a time-step with the PS method. Note that $\sqrt{g'/g} = 20$ implies that an HPM discretization of the unfiltered equation (1.1) would require a step-size twenty times smaller than the rigid-lid HPM method. This step-size restriction does not apply to the semi-implicit PS method.

Fig. 3.1 shows the time evolution of the baroclinic and barotropic vorticity fields over a time interval $[0, 150]$ using a step-size of $\Delta t = 0.125$. The corresponding results from the semi-implicit PS method with step-size $\Delta t = 0.025$ and initial $h_1^o \equiv 2 - h_2^o$ can be found in Fig. 4.1. In both cases, the smoothing operator S was applied to the gridded vorticity fields to average out fine scale vorticity filaments.

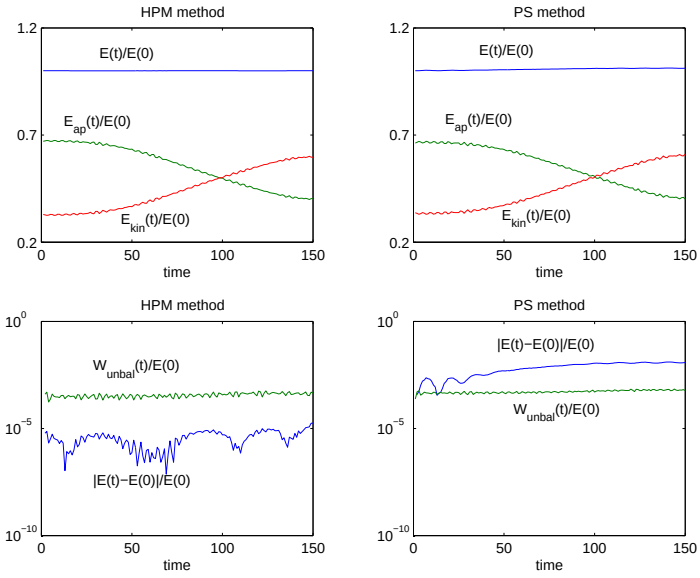

FIG. 5.1. *Diagnostic results.*

The vorticity fields are identical up to some small-scale differences over the whole time interval $[0, 150]$. A few diagnostic results for the rigid-lid and unconstrained simulations can be found in Fig. 5.1. More specifically, let $E(t_n)$ denote the total energy of the particle-mesh model,

$$E_{\rm kin}(t_n) \equiv \sum_{i=1}^{2} \sum_{k=1}^{N} \frac{1}{2m_i^k} \mathbf{v}_i^k(t_n) \cdot \mathbf{v}_i^k(t_n)$$

its kinetic energy (KE), and

$$E_{\rm ap}(t_n) \equiv \frac{c_0}{2} \sum_{p,q} \hat{h}_2^{pq}(t_n)[h_2^{pq}(t_n) - H_2]$$

its available potential energy (APE). For the incompressible rigid-lid model, we have $E(t_n) = E_{\rm kin}(t_n) + E_{\rm ap}(t_n)$. Up to a small potential energy contribution from the total layer-depth, this is essentially also true for the compressible two-layer model. We plot in Fig. 5.1 the scaled quantities $E(t_n)/E(t_0)$, $E_{\rm kin}(t_n)/E(t_0)$ and $E_{\rm ap}(t_n)/E(t_0)$ with $t_0 = 0$. Furthermore, we also monitor the norm of the unbalanced baroclinic velocity contributions

$$W_{\rm unbal}(t_n) \equiv \frac{1}{2} \|\Delta \mathbf{u}(t_n) - \Delta \mathbf{u}_{\rm thw}(t_n)\|_2^2,$$

with $\Delta \mathbf{u}_{\rm thw}$ defined by (4.1). Here all velocities are first approximated over the grid $\mathbf{x}^{pq}$ and then $\|.\|_2$ is to be understood as the discrete l_2-norm. In Fig. 5.1, we again plot the scaled variable

$W_{\rm unbal}(t_n)/E(t_0)$ and the numerically induced errors in total energy. The quasi-conservation of balanced motion for both methods, as manifested by the very small ratio $W_{\rm unbal}(t_n)/E(t_0)$, is particularly striking. The Rossby number for the simulation was $Ro \approx 0.1$. We also observe that the particle method conserves total energy much better.

We would like to point out that the given initial purely baroclinic state is persistent in the absense of the β-plane effect. Hence the break-up of the initial state into baroclinic and barotropic motion is triggered by $\beta \neq 0$.

6. Conclusions. Three dominant themes within geophysical fluid dynamics are (i) conservation, (ii) model reduction, and (iii) multi-scales. A simple model system that combines all three of these aspects is provided by the two-layer shallow-water equations. These equations are Hamiltonian, satisfy conservation laws of PV and circulation, can be simplified by filtering out surface gravity waves via the rigid-lid approximation, and geostrophic balance is of utmost importance for the long-time solution behavior in a small Rossby number regime. In the present paper, we have demonstrated how these ideas and concepts can be filtered through to the level of numerical methods. The proposed discrete particle-mesh method is Hamiltonian and conserves circulation/PV along the lines of [8, 5]. Furthermore, symplectic time-stepping guarantees maintenance of geostrophic balance as an adiabatic invariant [17]. Finally, the rigid-lid approximation is implemented as a holonomic constraint which allows significant increases in the attainable time-steps. We hope that the presented particle-mesh method can serve as a role model for further developments on more realistic model systems such as the primitive equations [19].

REFERENCES

[1] H.C. Andersen. Rattle: a 'velocity' version of the shake algorithm for molecular dynamics calculations. *J. Comput. Phys.*, 52:24–34, 1983.

[2] V.I. Arnold. *Mathematical Methods of Classical Mechanics.* Springer, New York, 2nd edition, 1988.

[3] G. Benetin and A. Giorgilli. On the Hamiltonian interpolation of near to the identity symplectic mappings with application to symplectic integration algorithms. *J. Statist. Phys.*, 74:1117–1143, 1994.

[4] C.K. Birdsall and A.B. Langdon. *Plasma Physics via Computer Simulations.* McGraw-Hill, New York, 1981.

[5] T.J. Bridges, P. Hydon, and S. Reich. Vorticity and symplecticity in Lagrangian fluid dynamics. Technical report, University of Surrey, Guildford, 2002.

[6] D.R. Duran. *Numerical Methods for Wave Equations in Geophysical Fluid Dynamics.* Springer-Verlag, New York, 1999.

[7] J. Frank, G. Gottwald, and S. Reich. The Hamiltonian particle-mesh method. In M. Griebel and M.A. Schweitzer, editors, *Meshfree Methods for Partial Differential Equations, Lecture Notes in Computational Science and Engineering*, volume 26, pages 131–142, Heidelberg, 2002. Springer.

[8] J. Frank and S. Reich. Conservation properties of smoothed particle hydrodynamics applied to the shallow-water equations. *BIT*, 43:40–54, 2003.

[9] E. Hairer and Ch. Lubich. The life-span of backward error analysis for numerical integrators. *Numer. Math.*, 76:441–462, 1997.

[10] R.W. Hockney and J.W. Eastwood. *Computer Simulations Using Particles.* Institute of Physics Publisher, Bristol and Philadelphia, 1988.

[11] L. O. Jay. Symplectic partitioned Runge-Kutta methods for constrained Hamiltonian systems. *SIAM J. Numer. Anal.*, 33:368–387, 1996.

[12] A.B. Langdon. Energy-conserving plasma simulation algorithms. *J. Comput. Phys.*, 12:247–268, 1973.

[13] B. Leimkuhler and R.D. Skeel. Symplectic numerical integrators in constrained Hamiltonian systems. *J. Comput. Phys.*, 112:117–125, 1994.

[14] H.R. Lewis. Energy-conserving numerical approximations for Vlasov plasmas. *J. Comput. Phys.*, 6:136–141, 1970.

[15] S. Reich. Symplectic integration of constrained Hamiltonian systems by composition methods. *SIAM J. Numer. Anal.*, 33:475–491, 1996.

[16] S. Reich. Backward error analysis for numerical integrators. *SIAM J. Numer. Anal.*, 36:475–491, 1999.

[17] S. Reich. Conservation of adiabatic invariants under symplectic discretization. *Appl. Numer. Math.*, 29:45–55, 1999.

[18] J.P. Ryckaert, G. Ciccotti, and H.J.C. Berendsen. Numerical integration of the cartesian equations of motion of a system with constraints: molecular dynamics of n-alkanes. *J. Comput. Phys.*, 23:327–341, 1977.

[19] R. Salmon. *Geophysical Fluid Dynamics.* Oxford University Press, 1999.

[20] J.M. Sanz–Serna and M.P. Calvo. *Numerical Hamiltonian Problems.* Chapman & Hall, 1994.